



Monochromatic Measurements of JPSS-1 VIIRS Polarization Sensitivity

Jeff McIntire¹, David Moyer², Steve Brown³, Eugene Waluschka⁴, Hassan Oudrari¹, and Xiaoxiong Xiong⁴

¹VCST / SSAI

²Aerospace Corporation

³NIST

⁴NASA GSFC

CALCON

Logan UT

August 23, 2016



Polarization Measurement Overview

JPSS-1 VIIRS polarization testing using the NIST T-SIRCUS

Performed at Raytheon El Segundo facility in December 2014

Purpose

- To make limited monochromatic measurements

- To compare to broadband measurements and validate model predictions

Analysis

- Data quality checks

- Perform Fourier analysis (Mueller matrix components)

- Derive DoLP and phase angle (wavelength dependent)

 - Compare to model predictions

- Integrate Fourier components over bandpass

 - Recalculate DoLP and phase angle

 - Compare to broadband measurements and model predictions

- Construct spectral responsivity functions

 - Investigate variation in centroid, bandwidth, and responsivity

JPSS-1 VIIRS

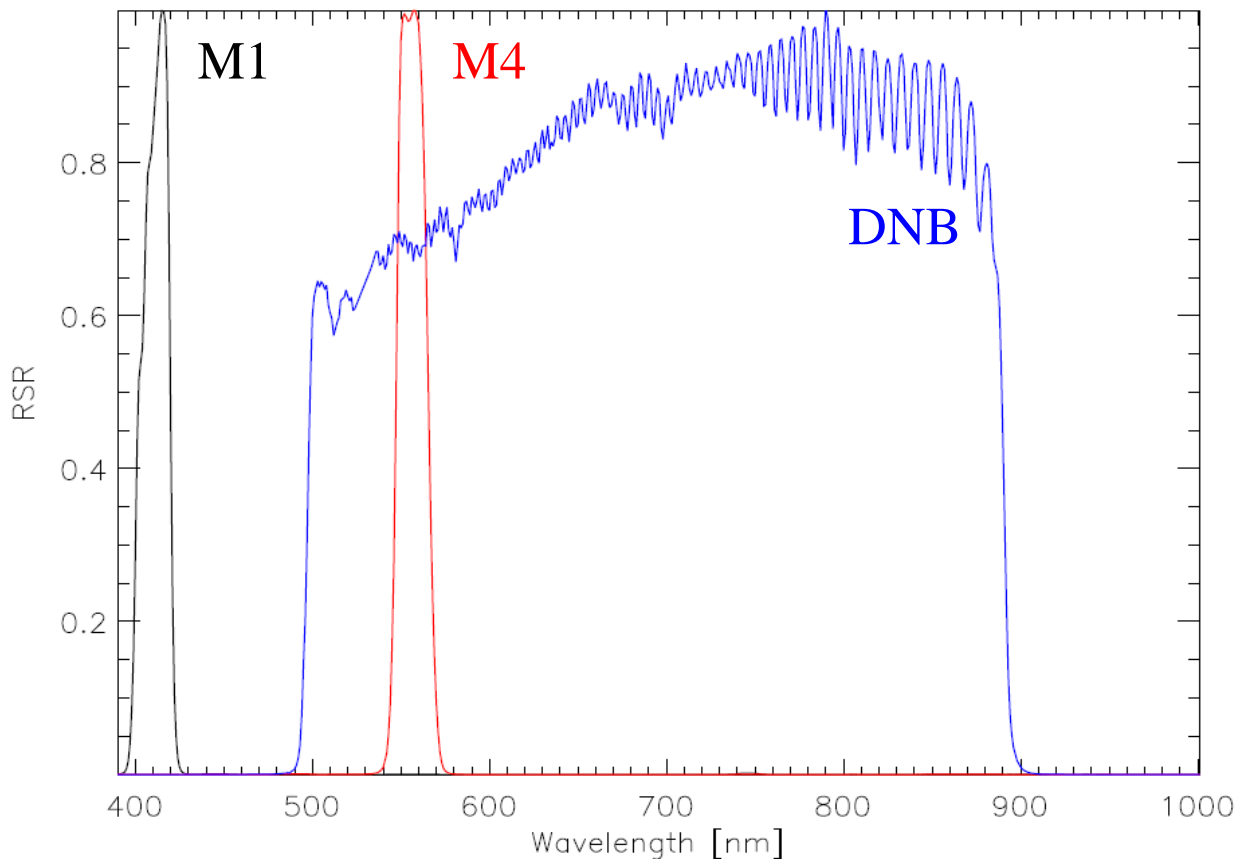
JPSS-1 VIIRS

JPSS-1 is the follow-on to SNPP

Bands measured are M1, M4, and DNB

Bands M1 and M4 have 16 Si-PIN detectors

DNB is a 4 stage CCD where the subpixels are aggregated into roughly the equivalent of 16 detectors at nadir



T-SIRCUS Test Setup

NIST T-SIRCUS

OPO pumped at 532 nm by a Nd:YVO₄ laser (397 – 424 nm and 543 – 565 nm)

Rhodamine 6G dye laser (566 – 572 nm)

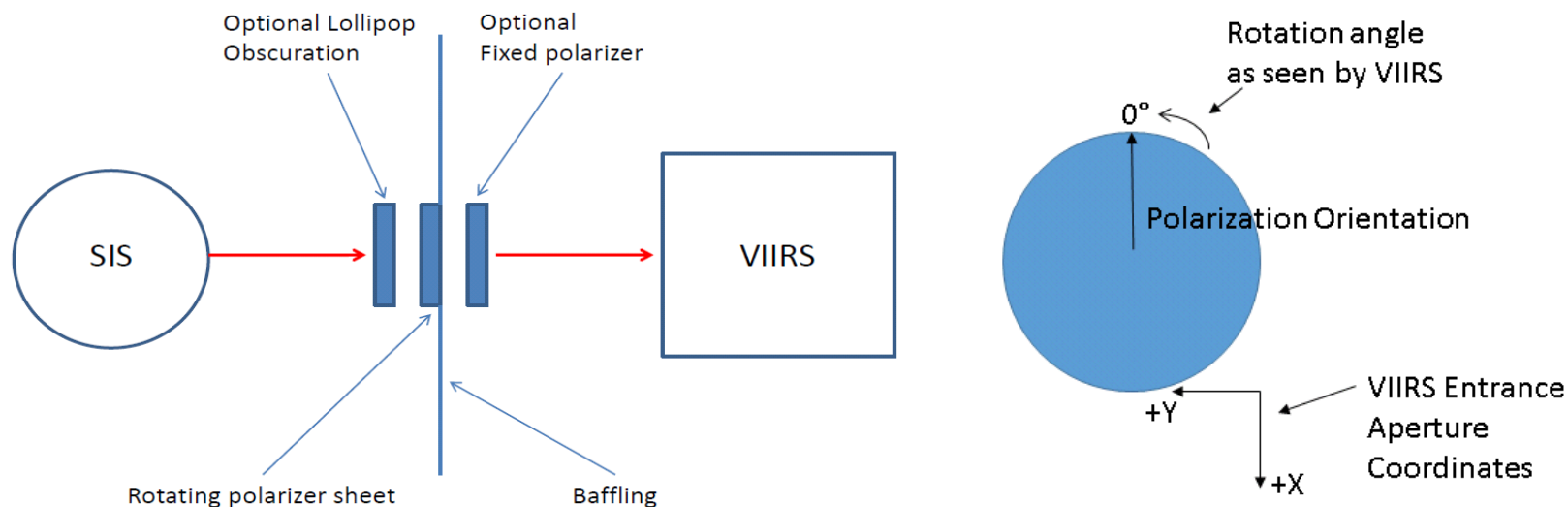
Laser bandwidths ~0.02 – 0.03 nm

Test Setup

Lasers used to feed a 100 cm SIS

BVONIR sheet polarizer mounted in a rotary stage (rotated from 0 to 180 degrees)

Lollipop obscuration and second, fixed polarizer sheet optional





T-SIRCUS Measurements

Measurements made by the NIST T-SIRCUS during polarization testing

Test Type	HAM Side	Scan Angle [degrees]	Target Band	Wavelengths [nm]
Stray Light – Dark	1	-8	M1, M4	NA
Stray Light – Lollipop	1	-8	M1 M4	415 559
Polarizer Efficiency	1	-8	M1 M4	401, 412, 420 559
Polarization Sensitivity	1	-8	M1	397, 400, 402, 404, 406, 408, 410, 413, 415, 417, 419, 421, 424
Polarization Sensitivity	1	+45	M1	397, 399, 402, 404, 406, 408, 410, 413, 415, 417, 419, 421, 424
Polarization Sensitivity	1	-8	M4	543, 546, 547, 548, 550, 552, 553, 555, 556, 558, 560, 561, 562, 564, 567, 569, 572
Polarization Sensitivity	0	-8	M4	543, 545, 547, 548, 550, 553, 556, 559, 562, 564, 567, 569, 572
Polarization Sensitivity	1	+45	M4	543, 545, 547, 549, 551, 552, 553, 554, 556, 558, 559, 561, 562, 564, 567, 569, 572



Methodology (I)

Data quality and processing

T-SIRCUS shutter open and closed times were matched to VIIRS scans (for each wavelength)

Out of family scans (with high standard derivations) were discarded

Scans for which the laser wavelength wandered were also discarded

Remaining shutter closed scans were averaged and then subtracted from the average shutter open scans (producing the dn)

Fourier analysis (wavelength dependent)

$$\frac{1}{2}c_0(\lambda) = \frac{1}{\pi} \int_0^{\pi} dn(\theta, \lambda) d\theta$$

$$C_2(\lambda) = \frac{2c_2(\lambda)}{c_0(\lambda)} = \frac{4}{\pi c_0(\lambda)} \int_0^{\pi} dn(\theta, \lambda) \cos(2\theta) d\theta \quad D_2(\lambda) = \frac{2d_2(\lambda)}{c_0(\lambda)} = \frac{4}{\pi c_0(\lambda)} \int_0^{\pi} dn(\theta, \lambda) \sin(2\theta) d\theta$$

Combine Fourier components (Mueller matrix components) into the DoLP and phase angle

$$DoLP(\lambda) = \frac{\sqrt{C_2^2(\lambda) + D_2^2(\lambda)}}{\sqrt{eff(\lambda)}} \quad phase(\lambda) = \frac{1}{2} \tan^{-1} \left[\frac{D_2(\lambda)}{C_2(\lambda)} \right]$$

Here the “eff” is the polarizer efficiency. The band and detector dependence are suppressed in the above equations. Spectral weighting is also applied to Fourier components.

Compare to model predictions (model predictions were analyzed using the above equations)

Methodology (II)

Fourier Analysis (band dependent)

Integrate wavelength dependent Fourier components over the M1 or M4 bandpass

$$C_2(B) = \frac{\int C_2(\lambda) RSR(\lambda) d\lambda}{\int RSR(\lambda) d\lambda} \quad D_2(B) = \frac{\int D_2(\lambda) RSR(\lambda) d\lambda}{\int RSR(\lambda) d\lambda}$$

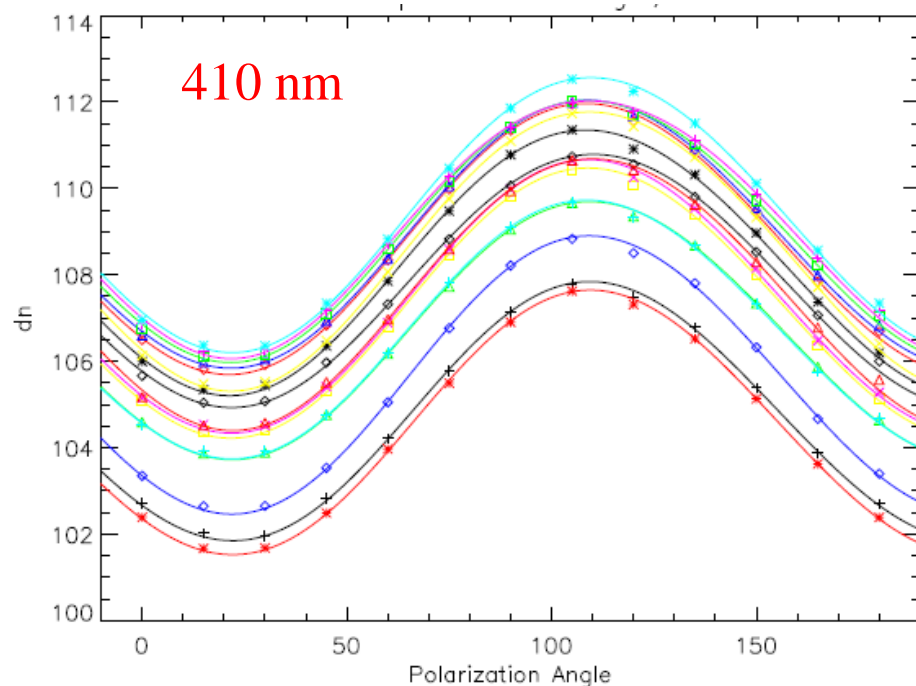
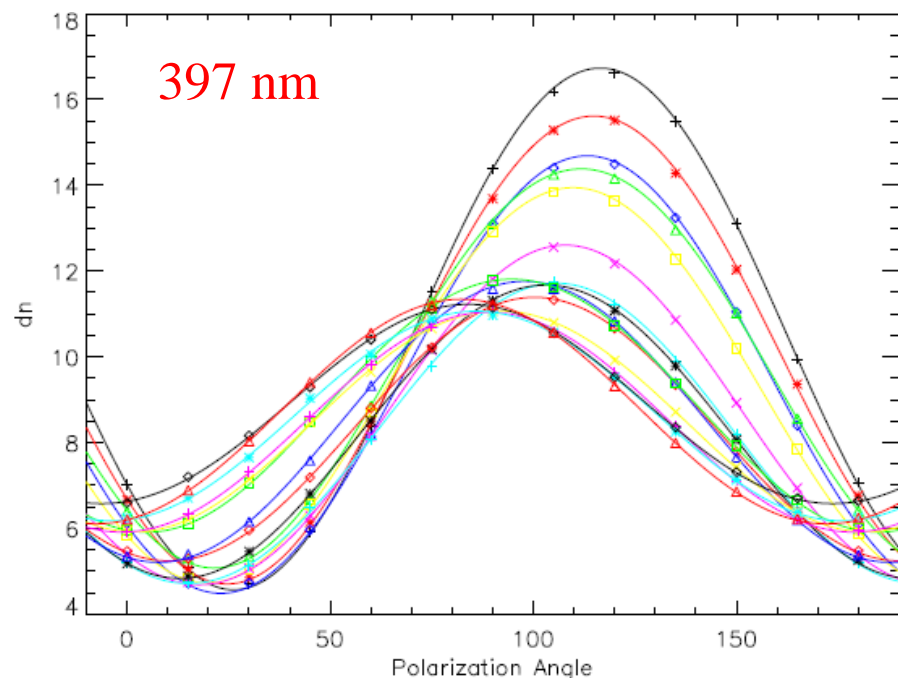
Combine Fourier components (Mueller matrix components) into the DoLP and phase angle

$$DoLP(B) = \frac{\sqrt{C_2^2(B) + D_2^2(B)}}{\sqrt{eff(B)}} \quad phase(B) = \frac{1}{2} \tan^{-1} \left[\frac{D_2(B)}{C_2(B)} \right]$$

Here the “eff” is the polarizer efficiency. Here the detector, scan angle and HAM side dependence are suppressed in the above equations.

Compare to broadband measurements and model predictions (analyzed using the above equations)

Modulation with Polarization Angle



+ 1 * 2 ◇ 3 △ 4 □ 5 × 6 + 7 ✖ 8 ◇ 9 △ 10 □ 11 × 12 + 13 ✖ 14 ◇ 15 △ 16

Fourier Analysis (M1, HAM 1, -8 degrees)

Modulation well described by the second order Fourier coefficients

Data filtering improved coefficient determination

4th order coefficients are negligible; 1st and 3rd order coefficients underdetermined

Variation in modulation (amplitude and phase) between detectors for some wavelengths

Variation of modulation (amplitude and phase) with wavelength

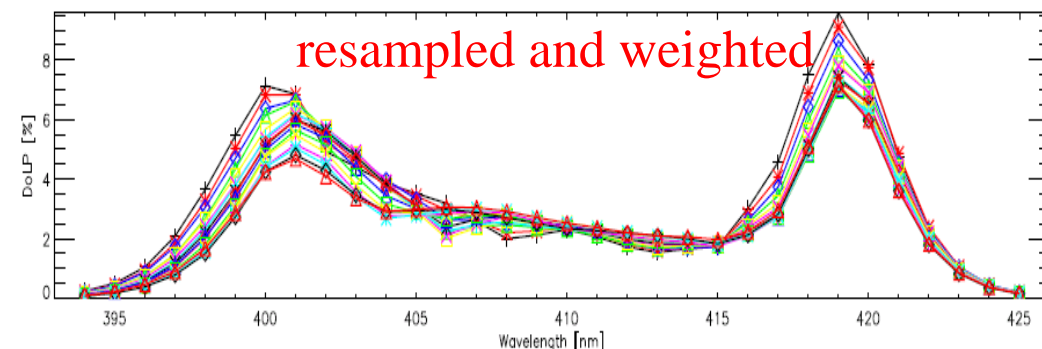
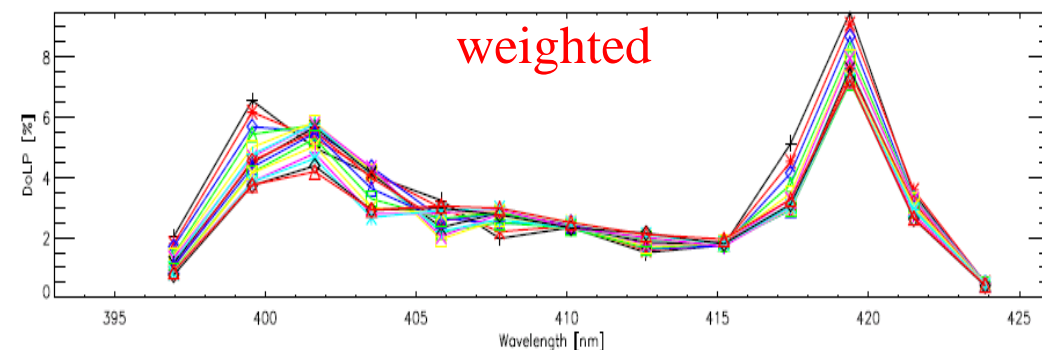
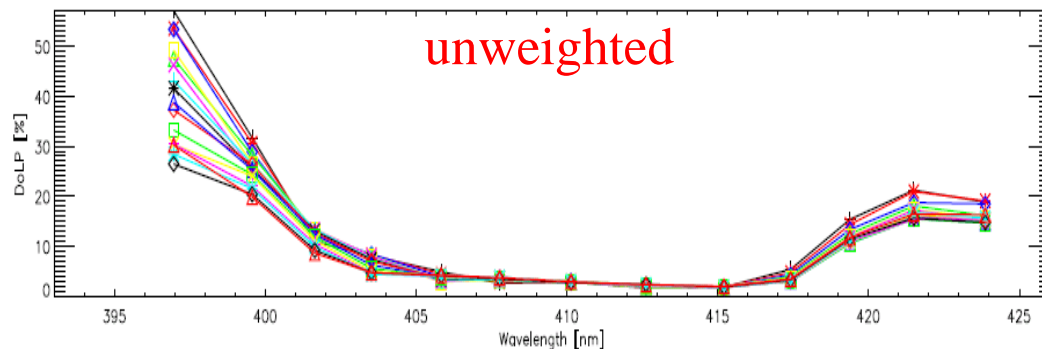
Measured DoLP

Measured DoLP M1, HAM 1, -8 degrees

Without spectral weighting, DoLP grows as move away from center of the bandpass (top plot)

Spectral weighting shows that DoLP is largest on the steep response zones of the bandpass (middle plot)

Resampling the Fourier coefficients to 1 nm and recomputing the DoLP and phase angle better defines the spectral dependence of the DoLP (bottom plot)



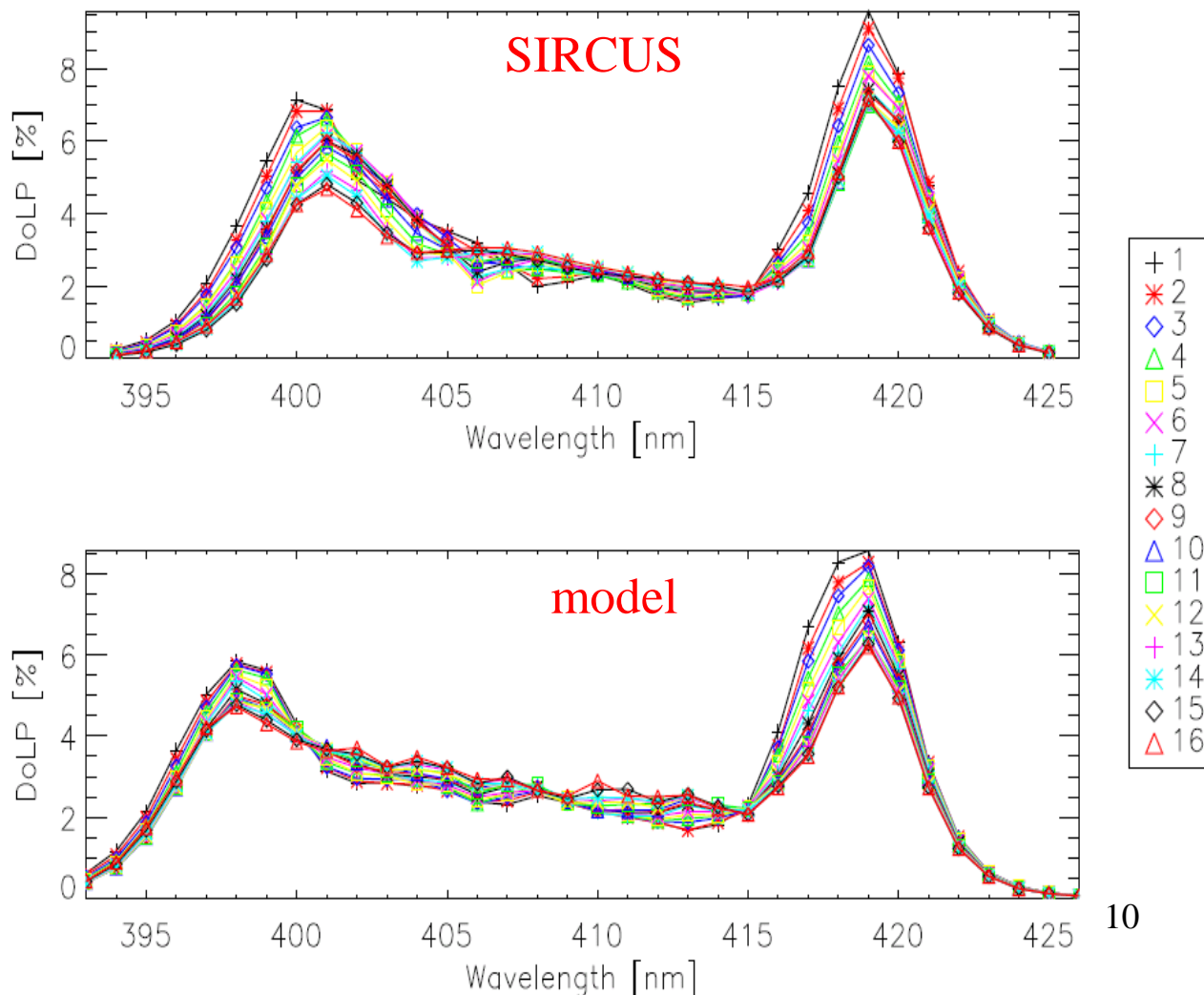
Measurement versus Model (I)

Weighted DoLP – M1, HAM 1, -8 degrees – measurement (top plot) and model (bottom plot)

Measurement and model agree in general shape of DoLP

Largest DoLP where the spectral response changes rapidly

Lower DoLP in the center of the bandpass



Measurement versus Model (II)

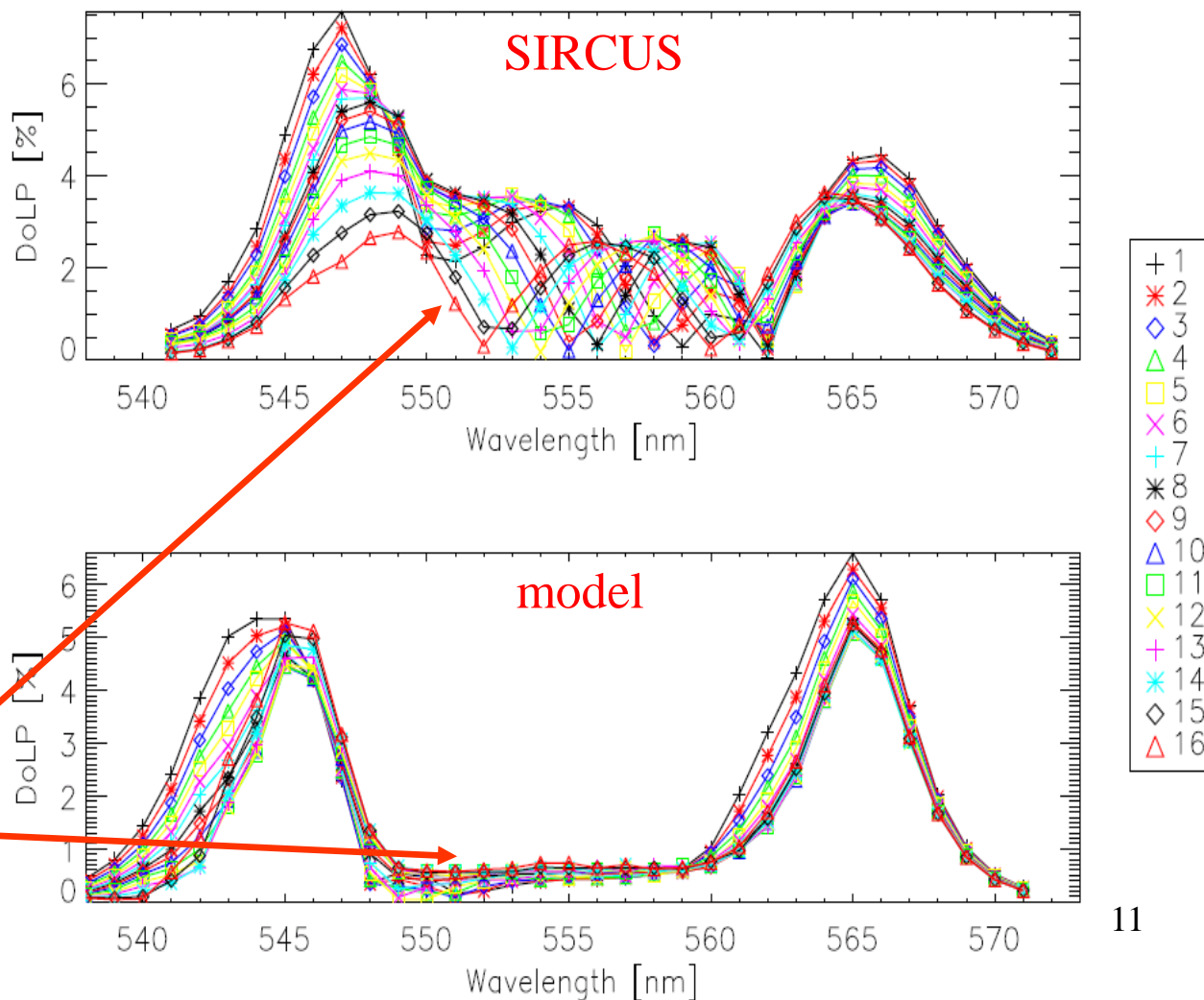
Weighted DoLP – M4, HAM 1, -8 degrees – measurement (top plot) and model (bottom plot)

Measurement and model agree in general shape of DoLP

Largest DoLP where the spectral response changes rapidly

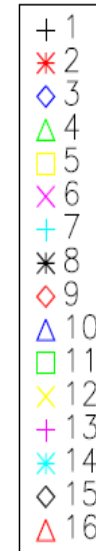
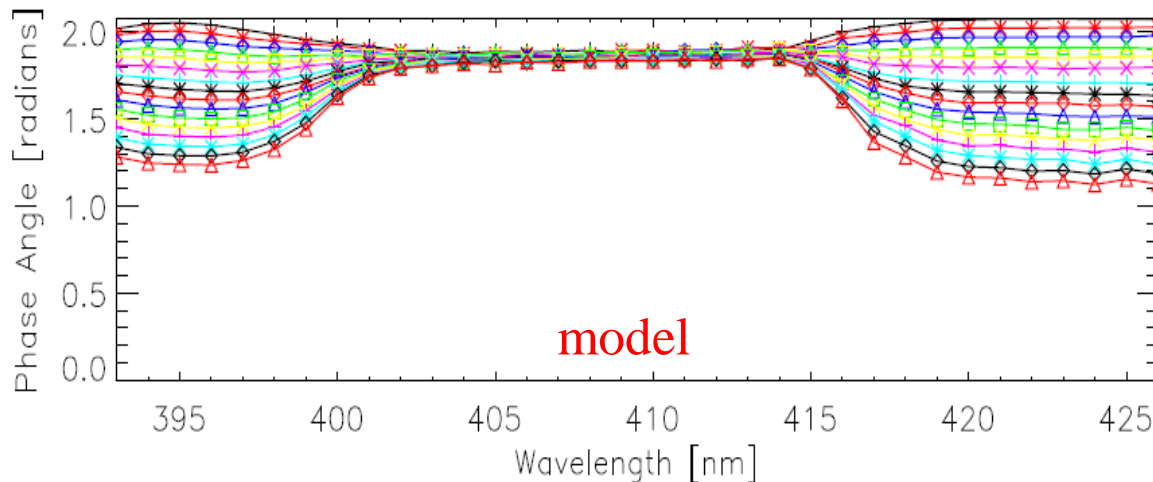
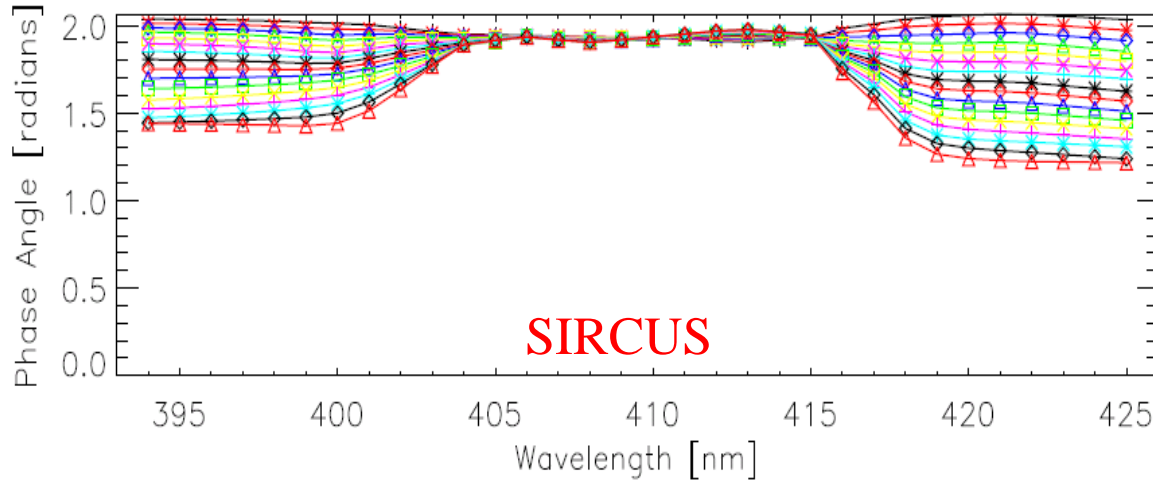
Lower DoLP in the center of the bandpass

However, phase change observed in measurement not predicted



Measurement versus Model (III)

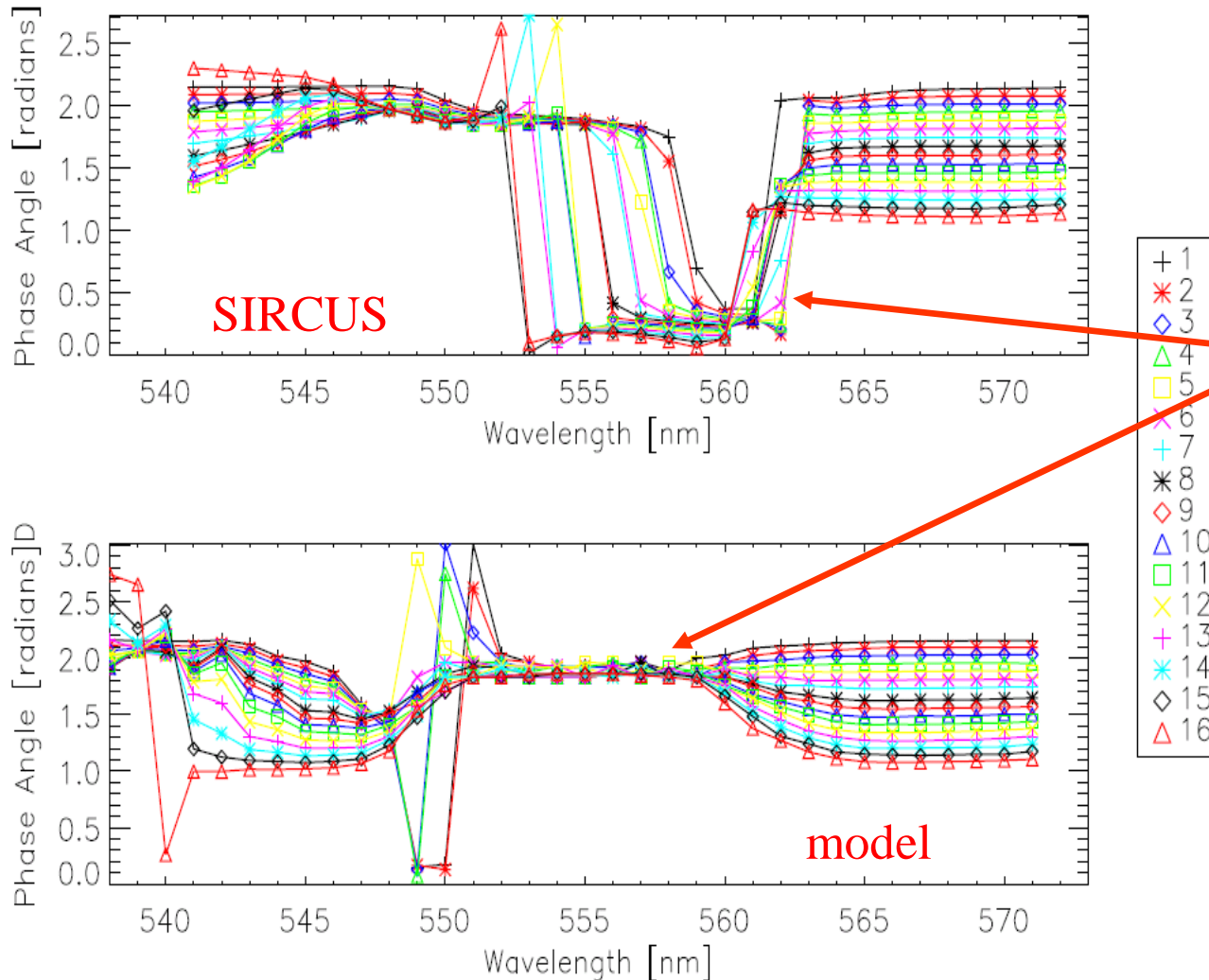
Phase Angle – M1, HAM 1, -8 degrees – measurement (top plot) and model (bottom plot)



Measurement and model agree in general shape of phase angle

Measurement versus Model (IV)

Phase Angle – M4, HAM 1, -8 degrees – measurement (top plot) and model (bottom plot)

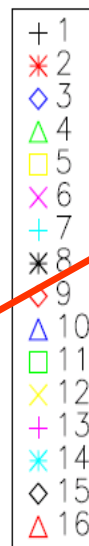
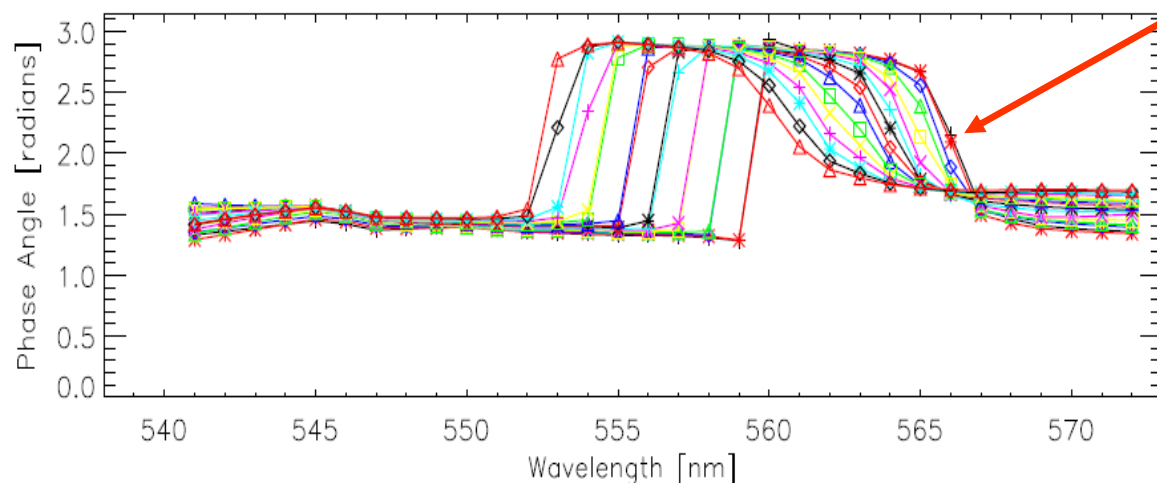
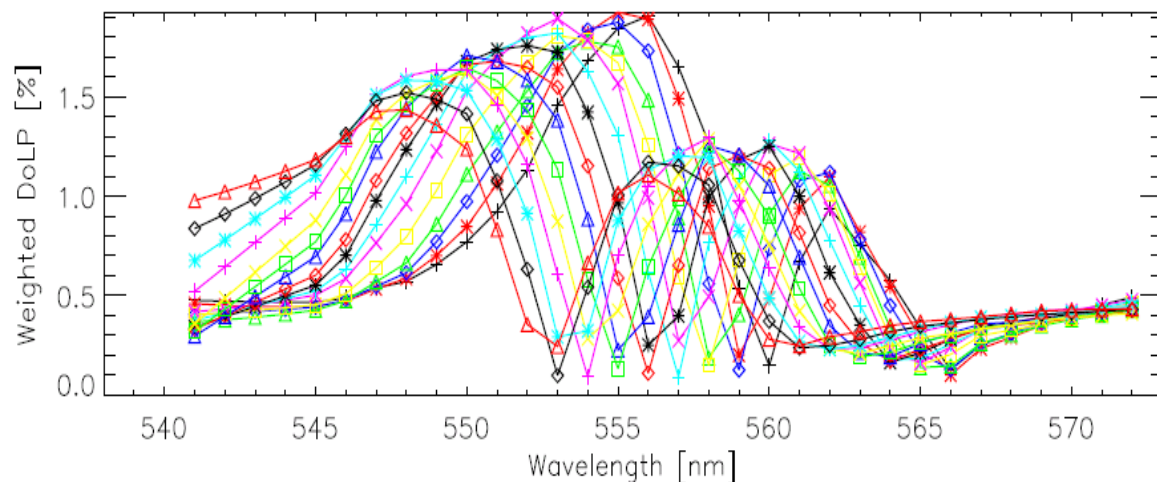


Phase angle change observed in the measurements was not predicted by the model

Phase angle changes by about 90 degrees in the center of the bandpass

Measurement versus Model (V)

Weighted DoLP and phase angle – DNB, HAM 1, -8 degrees



Limited DNB LGS measurements made in the M4 bandpass

Phase changes observed in M4 measurements also observed in the DNB

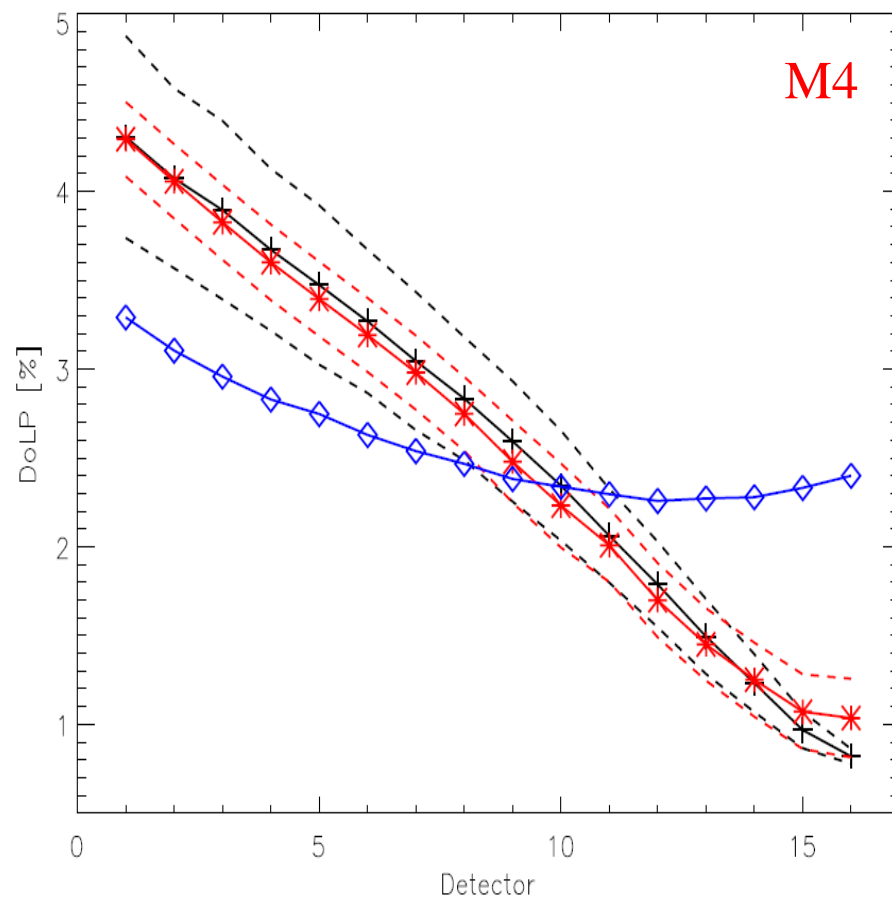
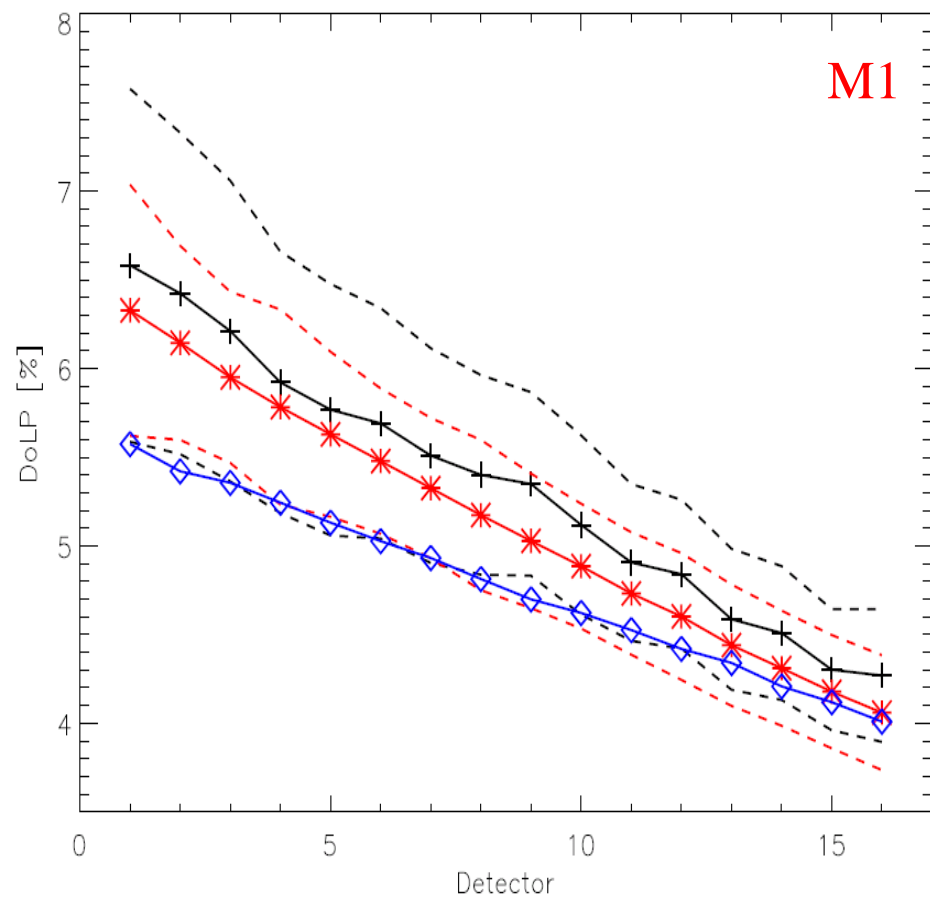
This indicates the phase angle shift is likely not caused by the spectral filters

Band Dependent DoLP

Band Dependent DoLP – SIRCUS measurement versus broadband measurement versus model

Black – SIRCUS; red – broadband; blue – model (HAM 1, -8 degrees)

Measurements agree within $k=2$ uncertainties



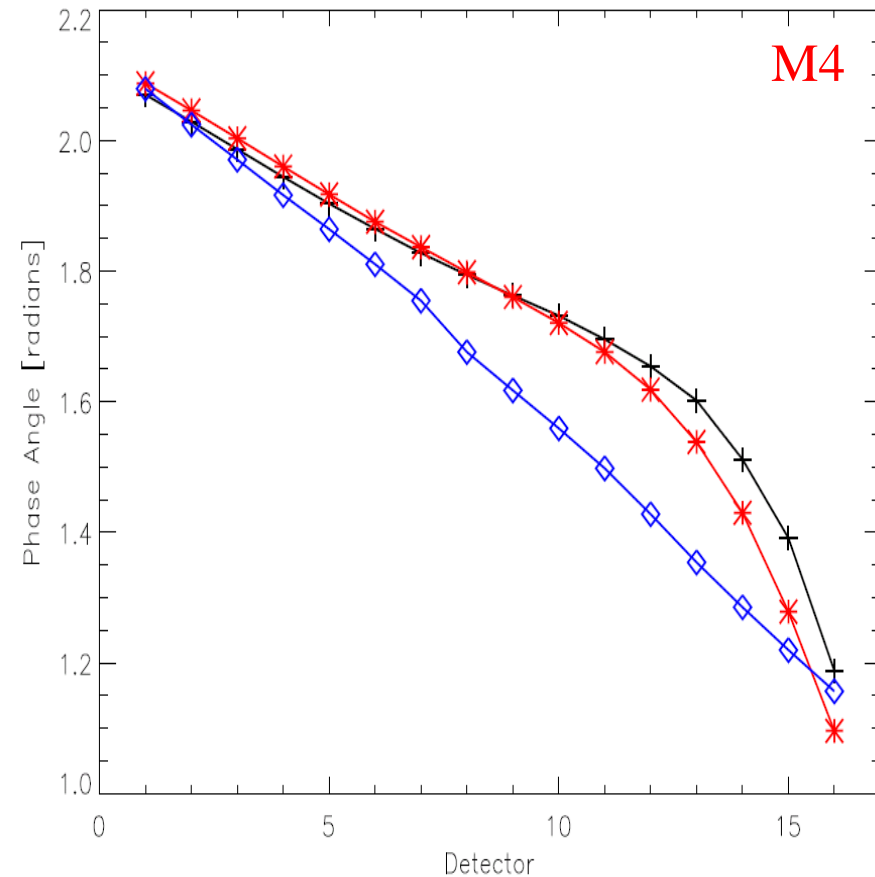
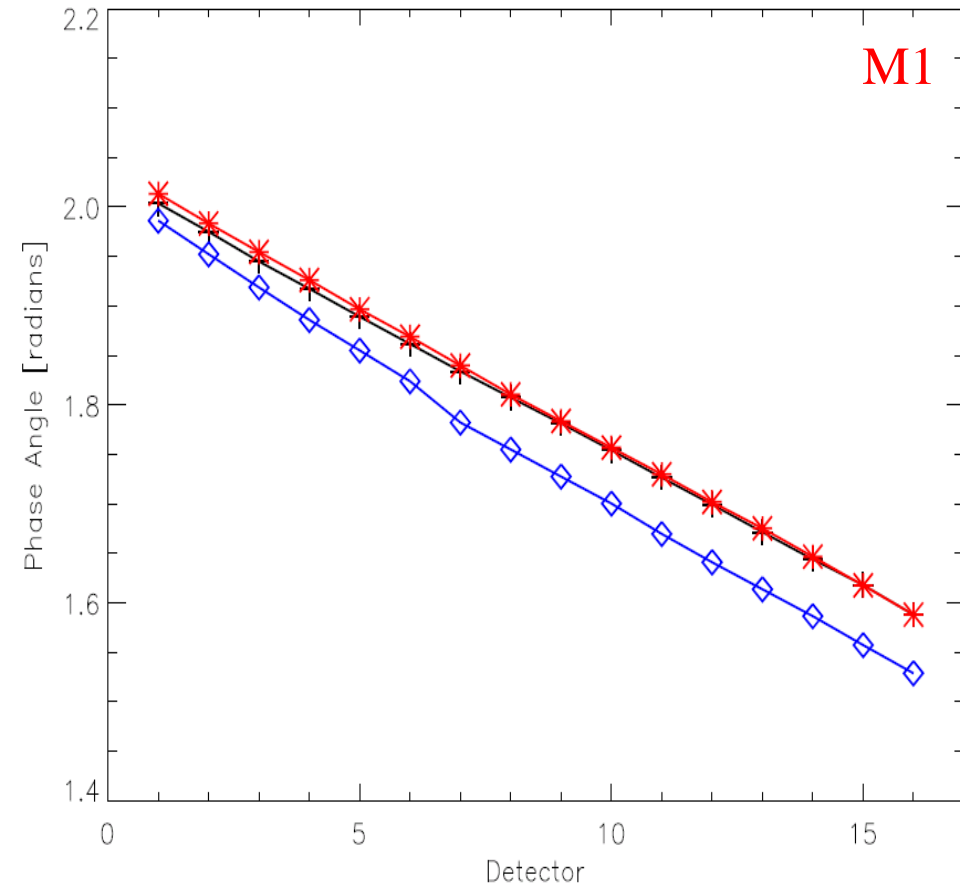


Band Dependent Phase Angle

Band Dependent Phase Angle – SIRCUS measurement versus broadband measurement versus model

Black – SIRCUS; red – broadband; blue – model (HAM 1, -8 degrees)

Measurements agree within 0.6 degrees (M1) and 6.5 degrees (M4)





Band Maximum DoLP

Band maximum DoLP for SIRCUS and broadband measurements as well as model

M1 comparison to model shows lower model values (but correct detector dependence)

Model may be using HAM side 0

M4 comparison to model also shows lower model values (detector dependence does not match)

Band	Test	HAM side	Scan Angle		Spec
			-8	+45	
M1	Broadband	1	6.33	6.16	3
	SIRCUS		6.73	6.69	
	Model		5.54	5.36	
M4	Broadband	1	4.29	3.99	2.5
	SIRCUS		4.47	4.17	
	Model		3.30	3.18	
	Broadband	0	4.18	3.88	
	SIRCUS		4.45	~	
	Model		3.30	~	

Methodology (III)

Absolute Spectral Response (ASR)

Define the ASR as the ratio of the response to the radiance

$$ASR(\lambda, \theta) = \frac{dn(\lambda, \theta)}{L(\lambda, \theta)}$$

for each measured wavelength and polarization state.

From the ASR, we can determine the responsivity, centroid wavelength and bandwidth as functions of polarization state

$$R(\theta) = \int d\lambda ASR(\lambda, \theta)$$

$$\lambda_c(\theta) = \frac{\int d\lambda \lambda ASR(\lambda, \theta)}{\int d\lambda ASR(\lambda, \theta)} = \frac{\int d\lambda \lambda ASR(\lambda, \theta)}{R(\theta)}$$

$$BW(\theta) = \frac{\int d\lambda ASR(\lambda, \theta)}{\max[ASR(\lambda, \theta)]_\lambda} = \frac{R(\theta)}{\max[ASR(\lambda, \theta)]_\lambda}$$

Methodology (IV)

Effects of different input spectra

SIRCUS measurements are equivalent to flat spectrum measurements

Model changes to ASR due to different input spectra (L_{source})

$$ASR'(\lambda, \theta) = ASR(\lambda, \theta) \frac{L_{source}(\lambda)}{L_{source}^{AVG}}$$

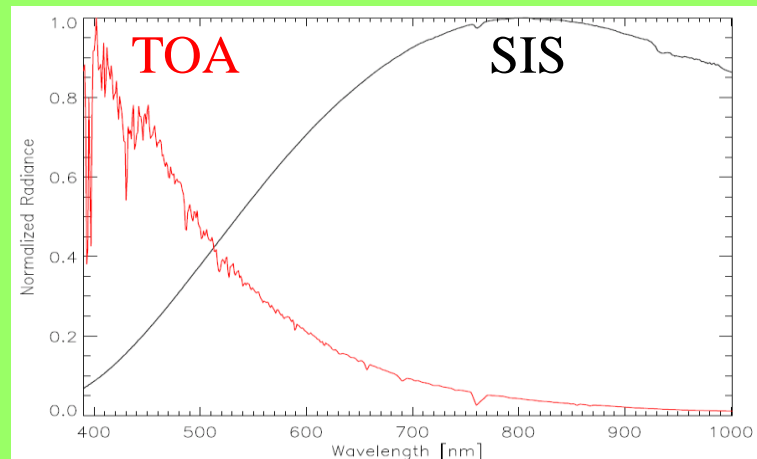
where L_{source}^{AVG} is the average spectral radiance is given by

$$L_{source}^{AVG} = \frac{\int d\lambda L_{source}(\lambda) ASR(\lambda, \theta)}{R(\theta)}$$

This only modifies the relative shape of the ASR, not the area; so changes in the centroid and bandwidth are investigated.

Two input spectra are used here:

- 1) a SIS spectrum to simulate prelaunch measurements
- 2) a TOA spectrum to simulate on-orbit conditions



Methodology (V)

Fourier Analysis

Assume that the radiance exiting the polarizer is independent of polarizer angle. The Fourier components can be rewritten in terms of the responsivity

$$C_2(B) = \frac{2}{\pi R(B)} \int_0^{\pi} d\theta \cos(2\theta) R(\theta) \quad D_2(B) = \frac{2}{\pi R(B)} \int_0^{\pi} d\theta \sin(2\theta) R(\theta)$$

Then the DoLP and phase angle can be rewritten in terms of the responsivity

$$DoLP(B) = \frac{2}{\pi R(\theta)} \frac{1}{\sqrt{eff(B)}} \left[\int_0^{\pi} d\theta_1 R(\theta_1) \int_0^{\pi} d\theta_2 R(\theta_2) \cos(2\theta_1 - 2\theta_2) \right]^{1/2}$$

$$phase(B) = \frac{1}{2} \tan^{-1} \left[\frac{\int_0^{\pi} d\theta \sin(2\theta) R(\theta)}{\int_0^{\pi} d\theta \cos(2\theta) R(\theta)} \right]$$

Compare results from this alternate approach to earlier approach.

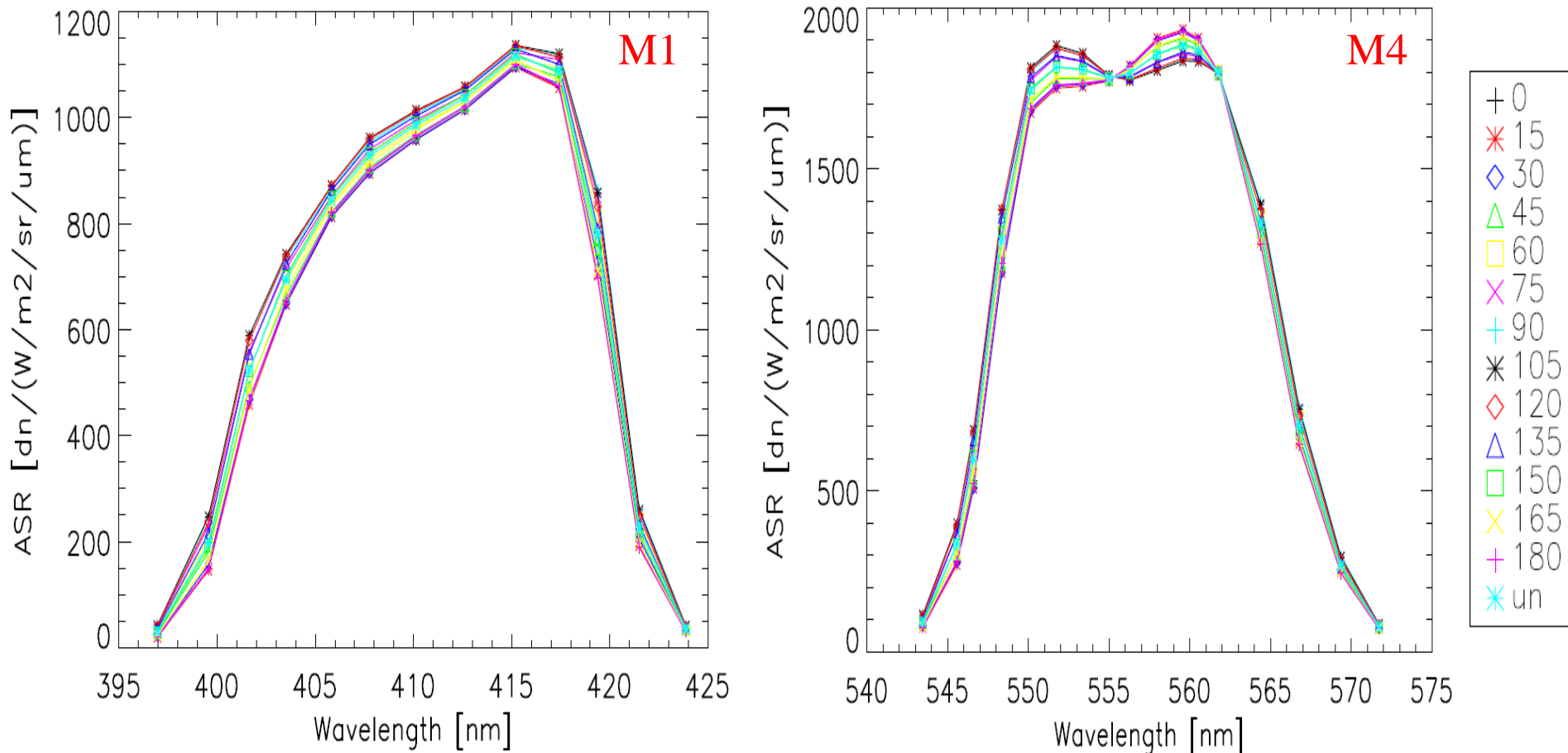
ASR (I)

ASR – M1 (left plot) and M4 (right plot) – detector 9, HAM 1, -8 degrees

Limited sampling of bandpass (13 or 17 measurements over bandpass)

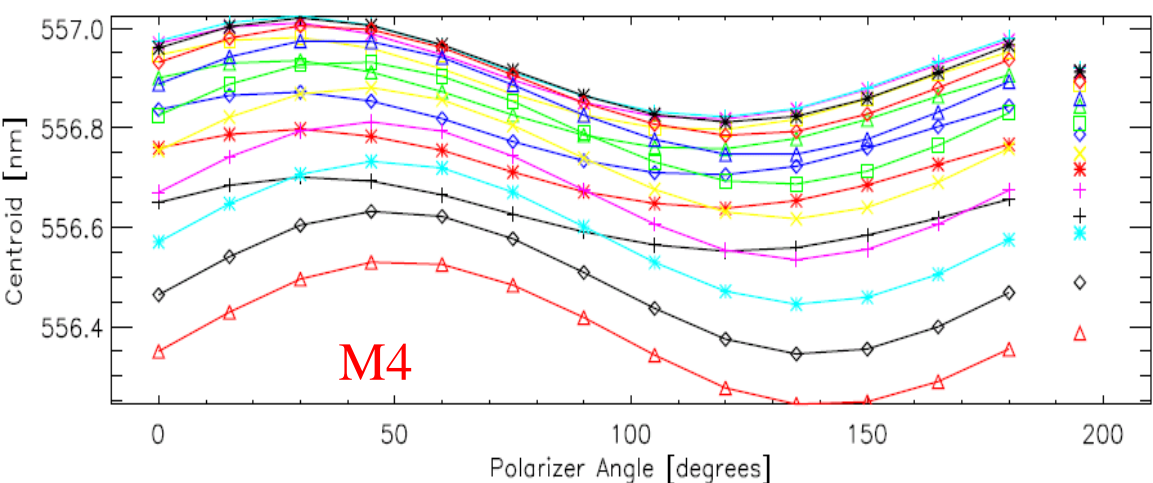
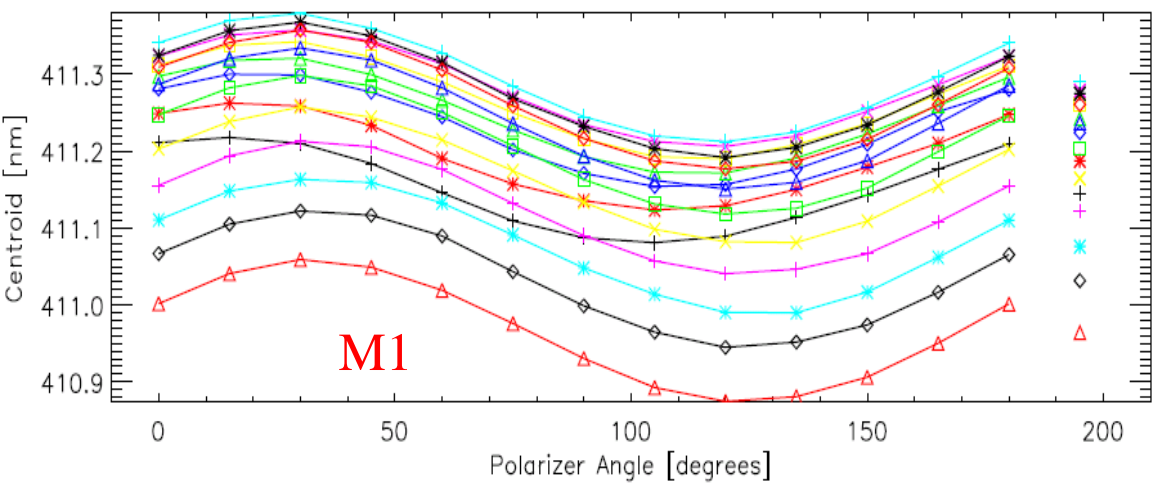
ASR shape varies with polarization state

Bandpass shifts with polarization state



Centroid (I)

Centroid – HAM 1, -8 degrees – M1 (upper plot) and M4 (lower plot)
 Disconnected data at 195 degrees represents the unpolarized case



- + 1
- * 2
- ◇ 3
- △ 4
- 5
- × 6
- + 7
- * 8
- ◇ 9
- △ 10
- 11
- × 12
- + 13
- * 14
- ◇ 15
- △ 16

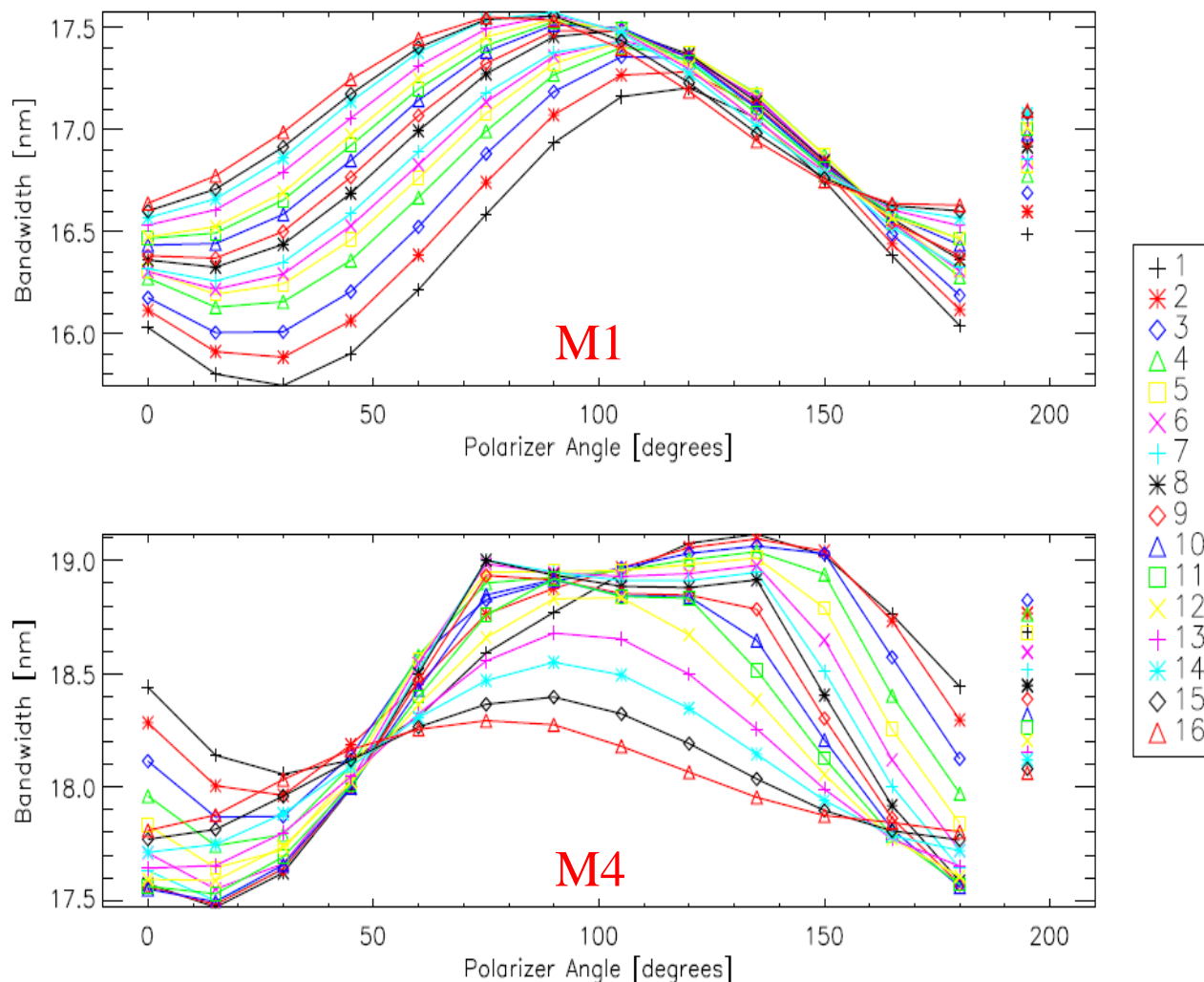
Centroids vary with polarizer angle with 2-cycle oscillation

Unpolarized measurement is roughly the average of the polarized measurements

Centroids vary with polarizer angle by up to:
 0.2 nm for M1
 0.3 nm for M4

Bandwidth (I)

Bandwidth – HAM 1, -8 degrees – M1 (upper plot) and M4 (lower plot)
 Disconnected data at 195 degrees represents the unpolarized case



Bandwidths vary with polarizer angle not always with 2-cycle oscillation – poor sampling of the bandpass for M4

Unpolarized measurement is roughly the average of the polarized measurements

Bandwidths vary by up to:
 1.5 nm for M1
 1.6 nm for M4

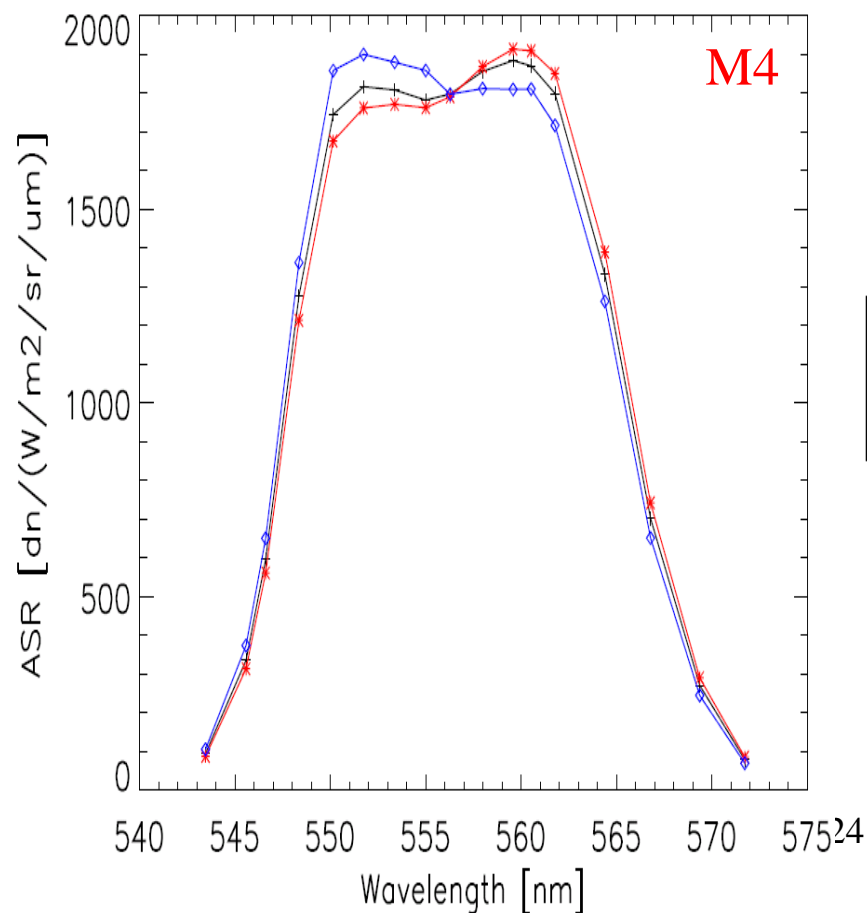
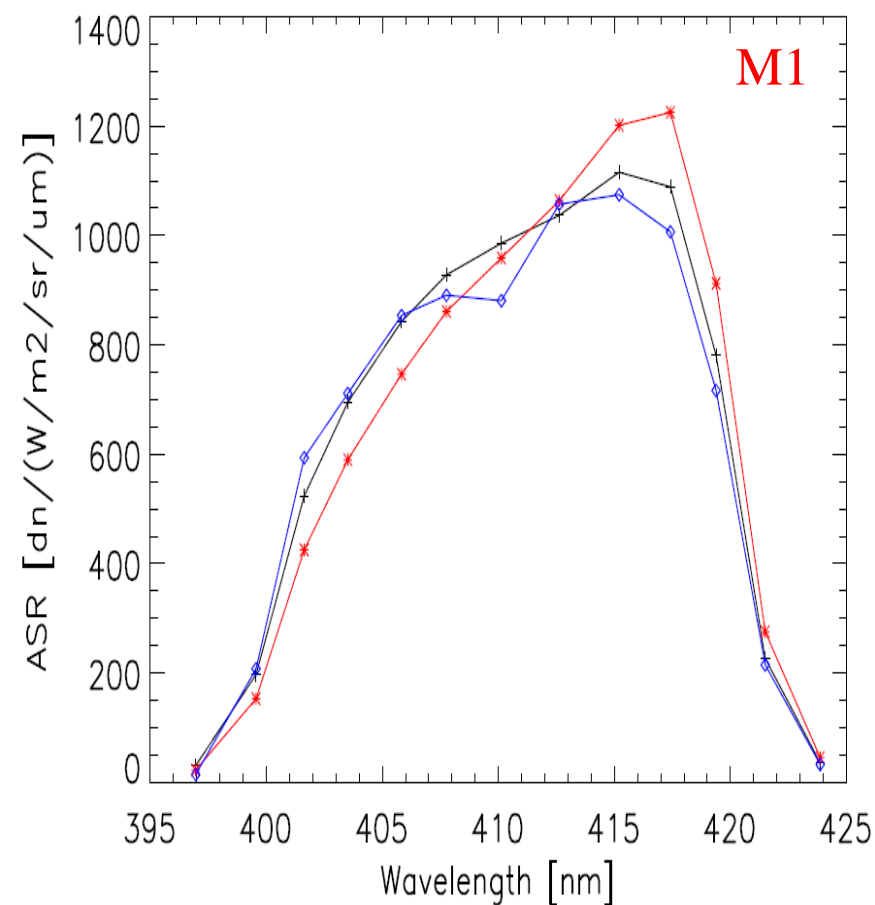
ASR (II)

ASR – M1 (left plot) and M4 (right plot) – detector 9, HAM 1, -8 degrees

Limited sampling of bandpass (13 or 17 measurements over bandpass)

Weighting the ASR by input spectra: SIS (simulate prelaunch) and TOA (simulate on-orbit)

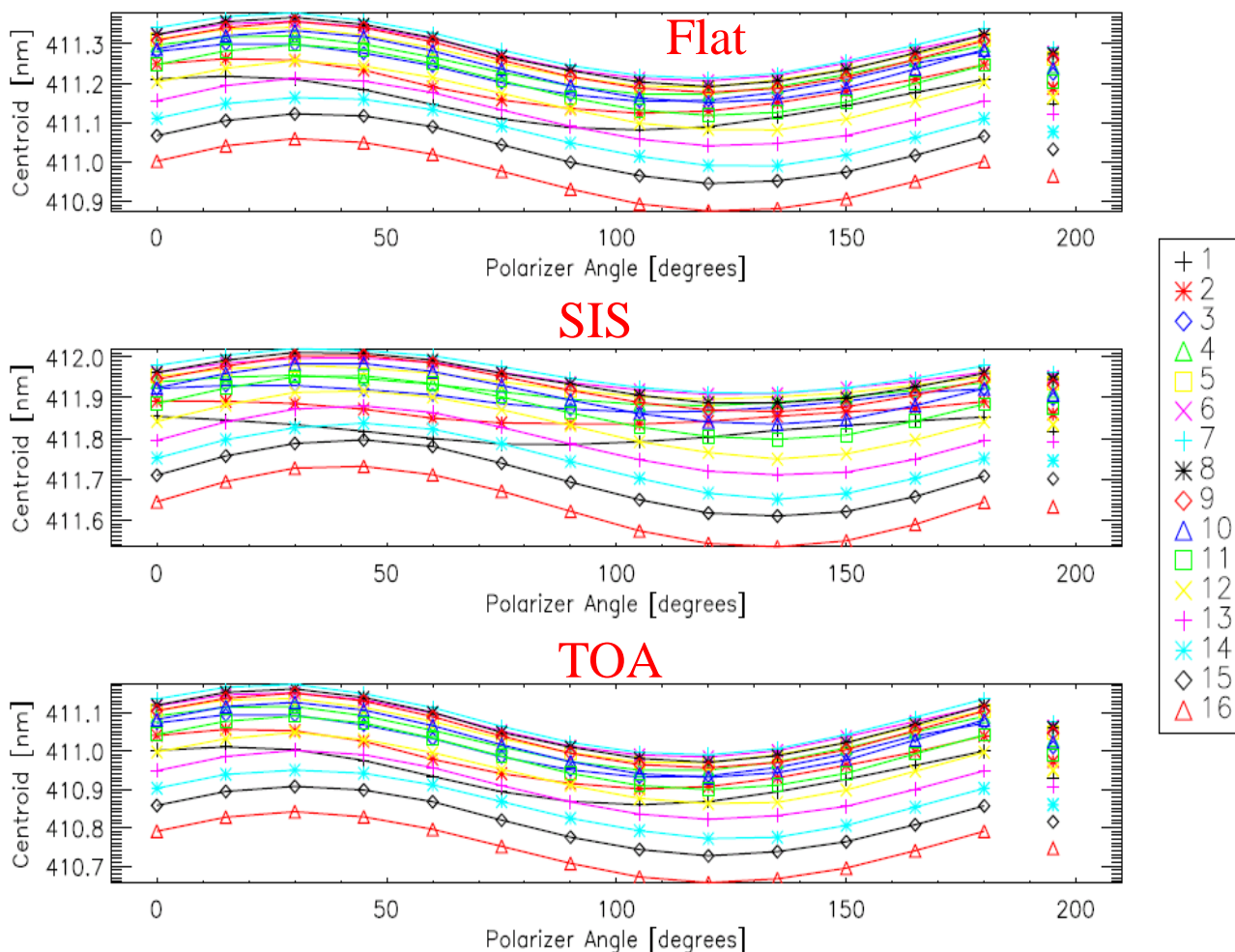
Shape and bandpass shift with polarization state



Centroid (II)

Centroid – HAM 1, -8 degrees – M1

Disconnected data at 195 degrees represents the unpolarized case
Centroid variations with input spectra (flat, SIS, and TOA)



Centroids vary with polarizer angle with 2-cycle oscillation

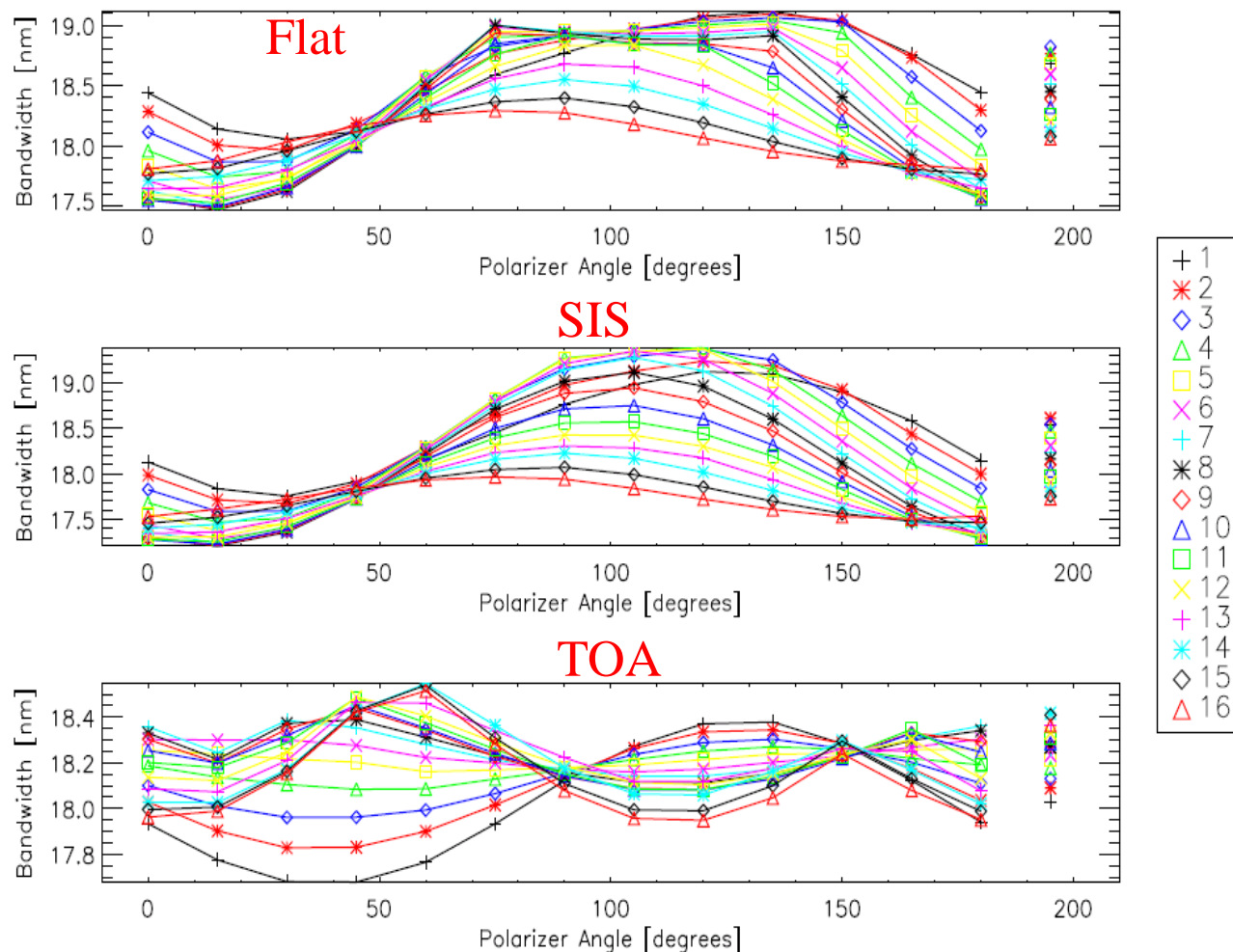
Unpolarized measurement is roughly the average of the polarized measurements

Centroids vary with polarizer angle by up to:
0.2 nm for M1 (all cases)
0.3 nm for M4 (all cases)

Bandwidth (II)

Bandwidth– HAM 1, -8 degrees – M4

Disconnected data at 195 degrees represents the unpolarized case
Bandwidth variations with input spectra (flat, SIS, and TOA)



Bandwidths vary with polarizer angle not always with 2-cycle oscillation – poor sampling of the bandpass for M4

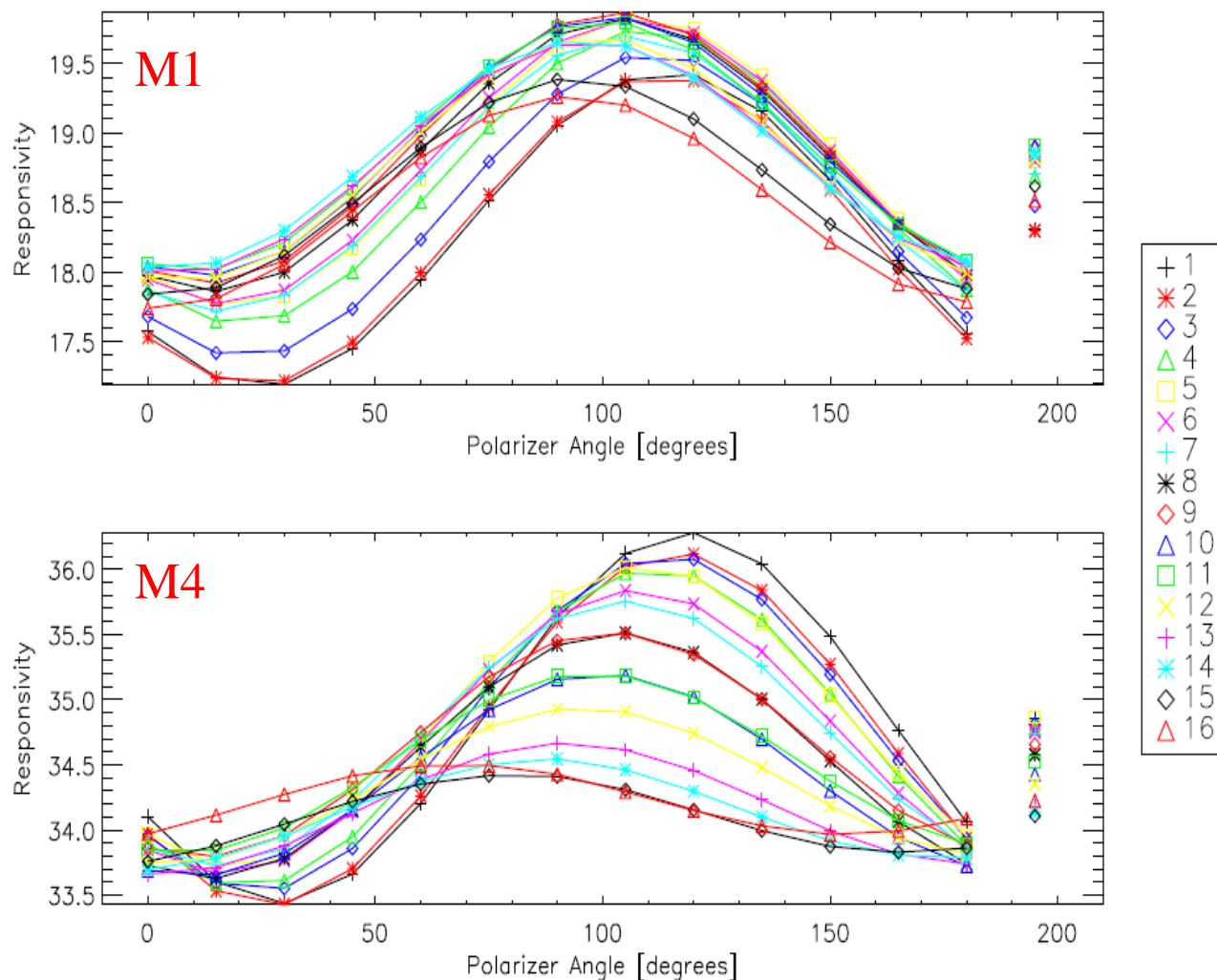
Unpolarized measurement is roughly the average of the polarized measurements

Bandwidths vary with polarizer angle by up to:
M1 (1.5 flat, 0.9 SIS, 1.5 TOA) nm
M4 (1.6 flat, 2.1 SIS, 0.8 TOA) nm

Responsivity

Responsivity – HAM 1, -8 degrees – M1 (upper plot) and M4 (lower plot)

Disconnected data at 195 degrees represents the unpolarized case



Responsivity varies with polarizer angle with 2-cycle oscillation

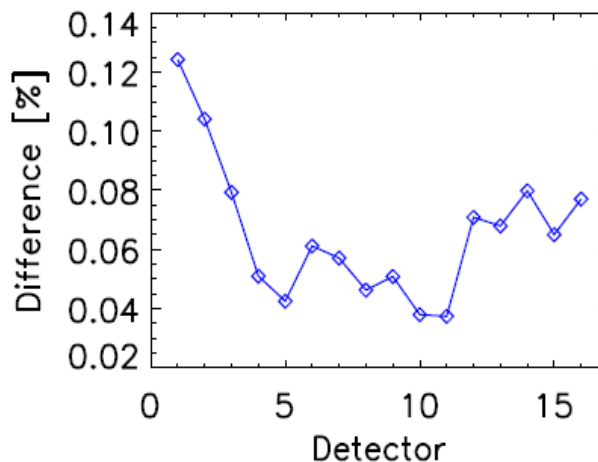
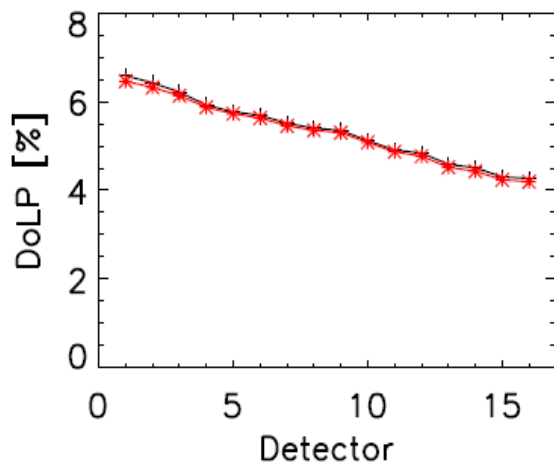
Unpolarized measurement is roughly the average of the polarized measurements

Responsivities vary with polarizer angle by up to:
6.1 % for M1
4.1 % for M4

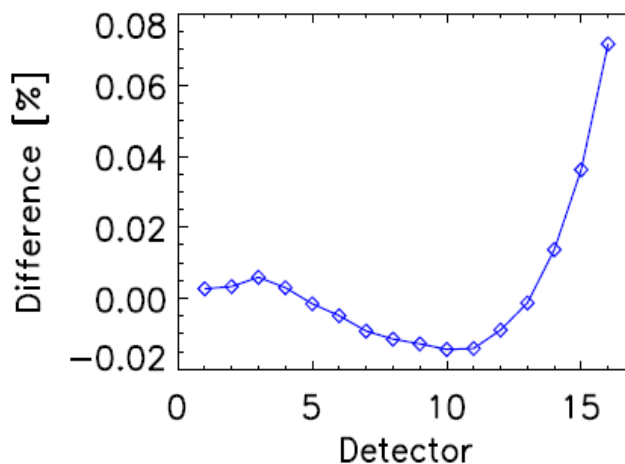
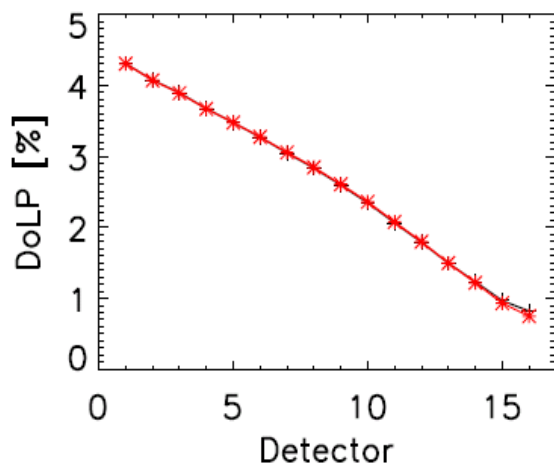
Method Comparison

Comparison of the two methods – HAM 1, -8 degrees

M1



M4



Methods should be equivalent

Agreement to within 0.13 % in DoLP and 3.4 degrees in phase angle



Centroid and Bandwidth Comparison

Band average centroids, bandwidths, and responsivities for SIRCUS testing

Spectral testing with SIRCUS measured both bandpasses with much finer sampling

Centroids are fairly consistent with input spectra

Some variation in bandwidth with input spectra

Responsivities tend to be lower than spectral testing (sampling)

Band	Spectra	Centroid	Bandwidth	Responsivity
M1	Flat	411.2	16.9	18.7
	SIS	411.9	15.5	--
	TOA	411.0	17.1	--
	Spectral	411.8	18.2	19.2
M4	Flat	556.8	18.4	34.5
	SIS	557.0	18.1	--
	TOA	556.5	18.3	--
	Spectral	556.9	18.1	34.7



Conclusions

T-SIRCUS polarization testing

Data analyzed and compared to broadband as well as model predictions

Model predicted that the edges of the bandpass were the largest contributors to the large polarization sensitivity

This was verified by the SIRCUS measurements

Some details not well described by the model (i.e. phase changes in M4)

Broadband and SIRCUS measurements generally agree well (to within 0.4% in DoLP)

Model agrees with broadband measurements for M1, but less well for M4

Spectral responsivity functions were constructed for each polarization state

Changes in centroid, bandwidth, and responsivity varied with polarization state

Acknowledgements:

Stellar Solutions (J.B. Young and J.K. McCarthy)

NIST (K.R. Lykke)

Raytheon test team (T.R. Wang)

Raytheon (E. Fest)

NASA (J. McCorkel and B. McAndrew)

VIIRS Cal/Val Government Team



Backup Slides